

Bayesian model comparison of Lorentz Invariance Violation using *Xiao et al* GRB spectral lag catalog

Shantanu Desai^{1,*}, Rajdeep Agrawal^{2,†} and Haveesh Singirikonda^{3‡}

^{1,2}*Department of Physics, Indian Institute of Technology, Hyderabad, Telangana-502285, India and*

³*Argelander-Institut für Astronomie, Auf dem Hügel 71, 53121 Bonn, Germany*

We use the spectral lag catalog of 46 short GRBs obtained by Xiao et al [1] between two fixed energy intervals in the source frame, to carry out an independent search for Lorentz Invariance violation (LIV). For this purpose, we use a power-law model as a function of energy for the intrinsic astrophysical induced spectral lags. The expansion history of the universe needed for the evaluation of LIV was obtained in a non-parametric method using cosmic chronometers. We use Bayesian model comparison to determine if the aforementioned spectral lags show evidence for LIV as compared to only astrophysically induced lags. We do not find any evidence for LIV, and obtain 95% c.l. lower limits for the energy scale of LIV to be 4×10^{15} GeV and 6.8×10^9 GeV for the linear and quadratic LIV models respectively.

I. INTRODUCTION

In many theoretical models beyond the Standard Model of Particle Physics, Lorentz Invariance is no longer an exact symmetry at energies close to the Planck scale ($E_{pl} \sim 10^{19}$ GeV), and the speed of light varies as a function of energy [2]

$$v(E) = c \left[1 - s_{\pm} \frac{n+1}{2} \left(\frac{E}{E_{QG}} \right)^n \right], \quad (1)$$

where $s_{\pm} = \pm 1$ corresponds to the sign of the Lorentz Invariance violation (LIV), corresponding to sub-luminal ($s_{\pm} = +1$) or super-luminal ($s_{\pm} = -1$). E_{QG} denotes the energy scale where LIV effects kick in, and n is a model-dependent term and is usually equal to one or two, corresponding to linear or quadratic LIV. The values of n for different phenomenological models of LIV are tabulated in [3].

For more than two decades Gamma-Ray Bursts (GRBs) have been a very powerful probe of LIV searches [3–27]. GRBs are single-shot explosions first detected in 1960s and have been observed over nine decades in energies from KeV-TeV range [28]. They are located at cosmological distances, although a distinct time-dilation signature in the light curves is yet to be seen [29]. GRBs are traditionally divided into two categories based on their durations, into long and short, with the demarcation boundary at two seconds [30]. Long GRBs are usually associated with core-collapse SN [31] and short GRBs with neutron star mergers [32]. There are however many exceptions to the aforementioned dichotomy, and many claims for additional GRB sub-classes have also been made [33, 34] (and references therein).

The observable used in LIV searches using GRBs consists of spectral lags, defined as the arrival time difference between high energy and low energy photons, and is positive if the high energy photons precede the low energy ones. A comprehensive review of all searches of LIV using GRB spectral lags (until 2021) can be found in our companion work [23] (A21, hereafter).

Most recently [27] (X22, hereafter) carried out a search for LIV using a catalog of GRB spectral lags from SWIFT-BAT and Fermi-GBM detectors. X22 constructed a catalog of spectral lags from 44 short GRBs and 21 long GRBs using both SWIFT-BAT and Fermi-LAT data. These lags were obtained between fixed source frame energy intervals of 15-70 keV and 120-250 keV, and were obtained using the novel Li-CCF method [1, 35]. This method utilizes the temporal information in the light curve and is agnostic to the details of the cross-correlation function. The spectral lag data from these 46 short GRBs were used to look for LIV. A constant source frame intrinsic lag was posited. Information theoretical criteria such as AIC and BIC [36] were used to test for the significance of a putative LIV signature compared to the null hypothesis of only intrinsic spectral lag. No such evidence was found and a 95% c.l. lower limit on E_{QG} from $10^{15} - 10^{17}$ GeV, depending on the value of s_{\pm} and the model assumed for LIV.

In this work we improve upon the analysis in X22 in multiple ways as outlined below:

*E-mail: shntn05@gmail.com

†E-mail: ep18btech11012@iith.ac.in

‡E-mail: haveesh.gss@gmail.com

- Firstly, instead of a constant intrinsic spectral lag, we assume the same phenomenological model for the intrinsic spectral lag as in A21 (and also [20, 37]).
- In the expression of LIV, instead of assuming the Λ CDM model, we use a non-parametric model-independent method for parameterizing the expansion history of the universe.
- We incorporate the uncertainty due to the bin widths of both the higher and lower energy bins in the likelihood used for the analysis.
- Finally, we use Bayesian model comparison for assessing the significance of LIV, instead of information theoretical considerations. Bayesian model comparison is more robust compared to AIC/BIC based tests of model comparison [36, 38, 39].

The outline of this manuscript is as follows. We discuss the dataset and analysis methodology in Sect. II. Our results are outlined in Sect. III and we conclude in Sect. IV.

II. DATASET AND ANALYSIS

A. Data

The dataset used for the analysis consists of spectral lags of 46 short GRBs collated in X22 using the Li-CCF technique. The spectral lags have been calculated using both Swift-BAT (44 GRBs) and Fermi-GBM (14 GRBs). X22 have shown that the spectral lags from both the detectors are consistent with each other within 1σ . For our analysis, we use the Swift derived spectral lags for 44 GRBs and the Fermi-GBM lags for two GRBs, namely 200826A and 170817A. The spectral lags were measured in a fixed rest frame energy intervals of 120-250 keV with respect to 15-70 keV.

B. Model for Spectral Lags

The analysis methodology used in this work is the same as that used in A21. We briefly recap this analysis, while more details can be found in A21. The first step in our analysis involves constructing a model for the observed spectral lags. This lag for a GRB located at redshift (z) can be written as the sum of two components:

$$\Delta t_{obs} = (1+z)\Delta t_{int}^{rest} + \Delta t_{LIV} \quad (2)$$

where Δt_{int}^{rest} is the intrinsic time delay due to astrophysical emission and Δt_{LIV} is the lag due to LIV. We use the following model for the intrinsic time lag (first proposed by [40]):

$$\Delta t_{int}^{rest} = \tau \left[\left(\frac{E}{keV} \right)^\alpha - \left(\frac{E_0}{keV} \right)^\alpha \right] \quad (3)$$

This intrinsic model was empirically determined by modelling the single-pulse properties of about 50 GRBs [41]. The LIV-induced lag is given by [42]:

$$\Delta t_{LIV} = - \left(\frac{1+n}{2H_0} \right) \left(\frac{E^n - E_0^n}{E_{QG,n}^n} \right) \frac{1}{(1+z)^n} \int_0^z \frac{(1+z')^n}{h(z')} dz' \quad (4)$$

where $E_{QG,n}$ is the quantum gravity scale, above which LIV is switched; E and E_0 correspond to the upper and lower energy intervals, equal to 42.5 keV and 185 keV, corresponding to the mid-point of the lower and upper energy bins, respectively. In Eq. 4, $n = 1$ and $n = 2$ corresponds to linear and quadratic LIV models, respectively. This parametric form for Δt_{LIV} corresponds to $s_+ = 1$ (cf. Eq. 1). In Eq. 4, $h(z) \equiv \frac{H(z)}{H_0}$ is the dimensionless Hubble parameter as a function of redshift. For the current standard Λ CDM model [43], $h(z) = \sqrt{\Omega_M(1+z')^3 + \Omega_\Lambda}$. This parametric form has been used in X22. In this work, similar to A21, we have evaluated the last term in the integrand non-parametrically using Gaussian Process Regression (GPR) [44]. The dataset used for GPR consists of cosmic chronometers [45]. We used the same chronometer dataset as in A21 (See also [46]). Details of this non-parametric regression using GPR can be found in A21 and some of our other works [46, 47].

C. Model Comparison

We evaluate the significance of any LIV using Bayesian Model Comparison. To evaluate the significance of a model (M_2) as compared to another model (M_1), one usually calculates the Bayes factor (B_{21}) given by:

$$B_{21} = \frac{\int P(D|M_2, \theta_2)P(\theta_2|M_2) d\theta_2}{\int P(D|M_1, \theta_1)P(\theta_1|M_1) d\theta_1} \quad (5)$$

where $P(D|M_2, \theta_2)$ is the likelihood for the model M_2 given the data D and $P(\theta_2|M_2)$ denotes the prior on the parameter vector θ_2 of the model M_2 . The denominator in Eq. 5 denotes the same for model M_1 . If B_{21} is greater than one, then model 2 is preferred over model 1 and vice-versa. The significance can be qualitatively assessed using the Jeffreys' scale [48]. More details on Bayesian model comparison can be found in various reviews [38, 39, 48] as well as some of our past works [36, 46, 49, 50] in addition to A21.

In this case, the model M_1 corresponds to the hypothesis, where the spectral lags are produced by only intrinsic astrophysical emission, whereas M_2 corresponds to the lags being described by Eq 4. To calculate the Bayes factor, we need a model for the likelihood (\mathcal{L}) described by

$$\mathcal{L} = \prod_{i=1}^N \frac{1}{\sigma_{tot} \sqrt{2\pi}} \exp \left\{ -\frac{[\Delta t_i - f(\Delta E_i, \theta)]^2}{2\sigma_{tot}^2} \right\}, \quad (6)$$

where Δt_i denotes the observed spectral lag data, σ_{tot} denotes the total uncertainty which is given by

$$\sigma_{tot}^2 = \sigma_t^2 + \left(\frac{\partial f}{\partial E}\right)^2 \sigma_E^2 + \left(\frac{\partial f}{\partial E_0}\right)^2 \sigma_{E_0}^2. \quad (7)$$

where f corresponds to the particular model been tested; σ_t is the uncertainty in the spectral lag; σ_E and σ_{E_0} correspond to the half-bin size of the upper and lower energy intervals, which are equal to 27.5 keV and 65 keV, respectively. The last ingredient we need to evaluate Eq. 5 are the priors for the three models. We have used uniform priors for α and τ , and log-uniform priors on E_{QG} . The prior ranges for all these parameters can be found in Table II.

III. RESULTS

Similar to A21, we used the Nested Sampling package `dynesty` [51] for calculating the Bayesian evidences. The 68% and 90% marginalized credible intervals for the model parameters obtained from this sampling can be found in Figs. 1, 2, 3 for the null hypothesis, linear LIV model, and quadratic LIV model, respectively. The Bayes factor for the linear and quadratic LIV models compared to the null hypothesis, as well as the χ^2/dof for all the three models can be found in Table II. We see that the Bayes factors for both the LIV hypotheses compared to the null hypothesis of only intrinsic astrophysical emission is close to one, indicating that there is no evidence for LIV. The χ^2/dof for all the three models is close to one, indicating that all of them provide reasonably good fits.

We do not get closed contours for E_{QG} for both the LIV models. Therefore, we set lower limits using the same method as A21, following the prescription in [6], which we outline below.

$$\frac{\int_{E_{QG}}^{E_\infty} L_{marg}(x) dx}{\int_{E_0}^{E_\infty} L_{marg}(x) dx} = 0.68, \quad (8)$$

where $L_{marg}(x)$ is the likelihood obtained after marginalizing over the nuisance parameters (τ and α), and $E_\infty = 10^{19} GeV$, corresponding to the Planck scale. To evaluate Eq. 8, we use the `dynesty` package and the same priors as in Table I. The 95% c.l. lower limit on E_{QG} is then given by for $E_{QG} > 4 \times 10^{15}$ GeV and $E_{QG} > 6.8 \times 10^9$ GeV for linear LIV and quadratic LIV, respectively.

IV. CONCLUSIONS

In a recent work, X22 carried out a search for LIV from the spectral lags of 46 short GRBs between two fixed energy intervals in the source frame: 120-250 keV and 15-70 keV. This work complements the numerous studies of LIV previously done using long GRBs.

Parameter	Prior	Minimum	Maximum
α	Uniform	-0.5	0.5
τ	Uniform	-5	5
$\log_{10}(E_{QG}/GeV)$	Uniform	6	19

TABLE I: Priors used for the calculation of Bayesian evidence for all the three models considered hitherto.

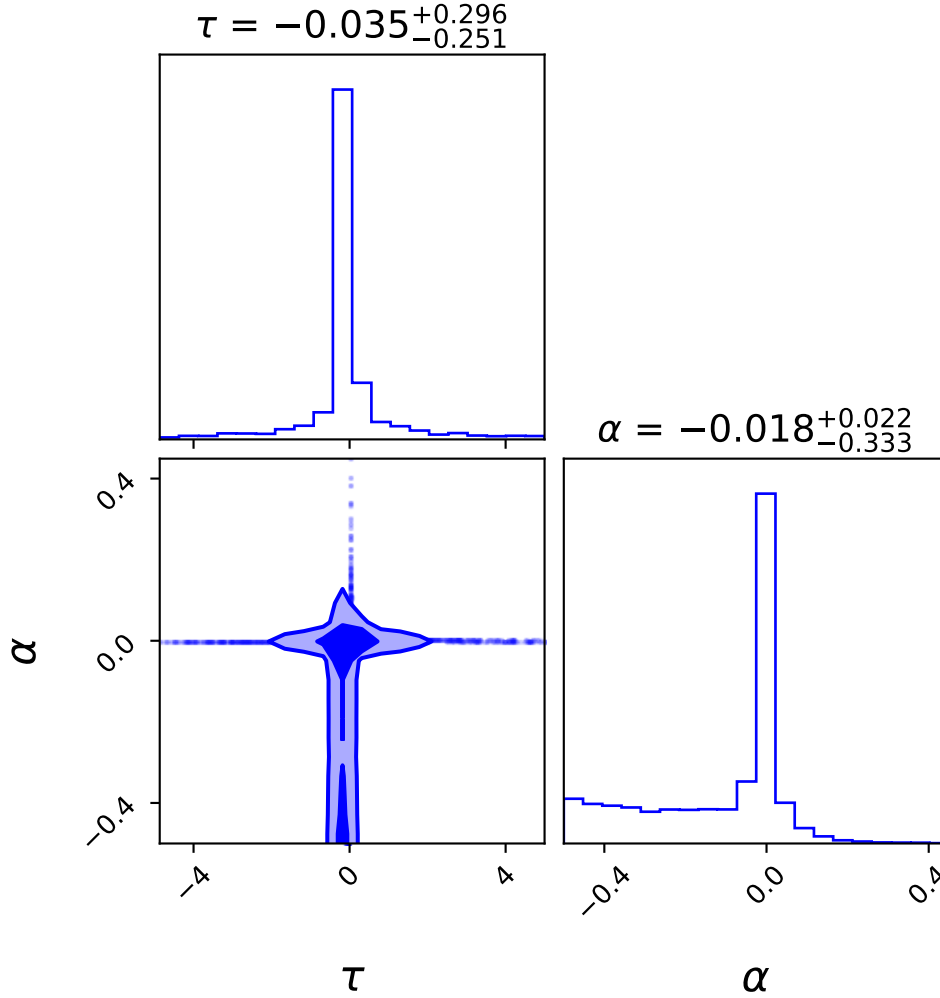


FIG. 1: The marginalized 68% and 90% credible regions for the parameters of the null hypothesis of the observed time lags being only due to intrinsic emission. The marginalized best-fit estimates for τ and α are depicted in the figure.

	No LIV	(n=1) LIV	(n=2) LIV
χ^2/DOF	55.8/44	51.3/43	52.6/43
Bayes Factor	-	0.3	1.1

TABLE II: Bayesian statistical significance of the two LIV models as compared to the null hypothesis of only intrinsic emission. We also provide the χ^2/DOF for all the three models, where DOF is equal to the total number of data points minus the number of free parameters. The Bayes factor shows negligible evidence for LIV for both the models. The χ^2/DOF show reasonable fits for all the models.

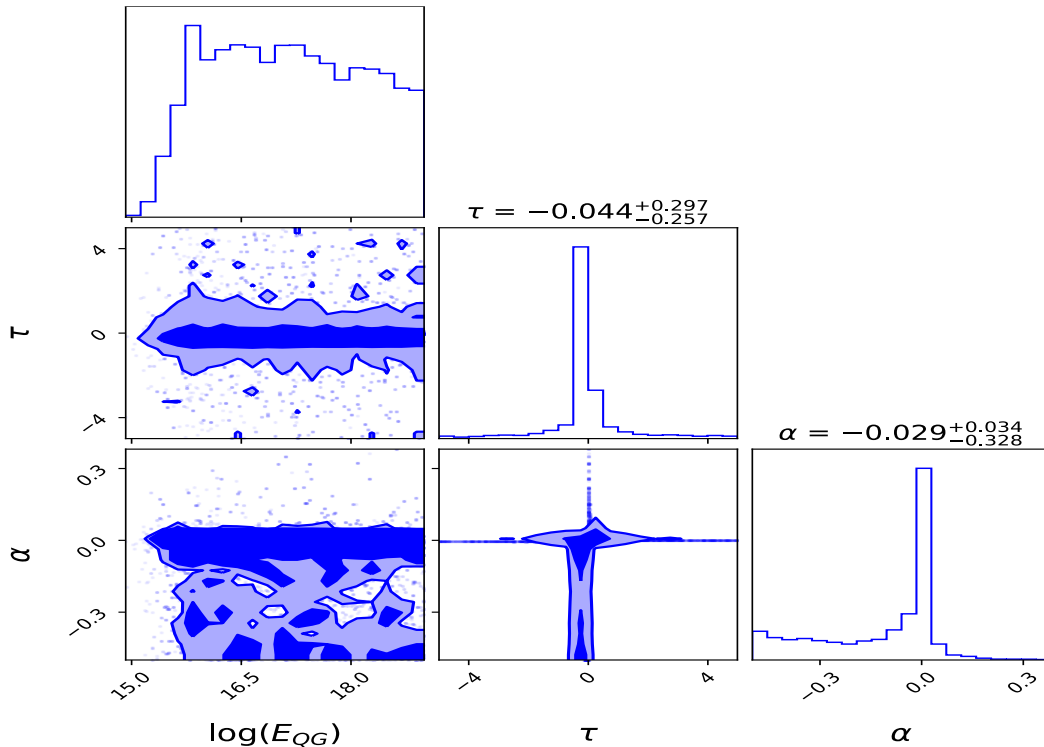


FIG. 2: The marginalized 68% and 90% credible regions for the linear LIV model, corresponding to $n = 1$ in Eq. 4. Since, no closed contour for E_{QG} is obtained, we only set lower limits on E_{QG} , given by $E_{QG} > 4 \times 10^{15}$ GeV at 95% c.l.

In this work, we carried out an independent search for LIV using the aforementioned spectral lag data following the same methodology as our previous work [23]. Instead of assuming a constant model for the intrinsic emission as in X22, we used the same power-law model as a function of energy for the intrinsic emission as in A21. We parameterized the expansion history of the universe (needed to evaluate the LIV-induced lag) in a model-independent way using cosmic chronometers. We search for both linear and quadratic LIV violation.

The marginalized credible intervals for the parameters of all three of our models can be found in Fig. 1, Fig. 2, and Fig. 3. Since we do not get closed contours for E_{QG} , we set 95% c.l. lower limits using the same method as in [6]. We find that $E_{QG} > 4 \times 10^{15}$ GeV and $E_{QG} > 6.8 \times 10^9$ for linear LIV and quadratic LIV, respectively.

The χ^2/dof for all the three models are close to one (cf. Table II) indicating that all the models provide an adequate description of the data. The results of Bayesian model comparison for the two LIV hypotheses compared to the null hypothesis are shown in Table II. We find that the Bayes factors are close to one, indicating that there is no evidence that spectral lags are induced due to LIV. Note that this is in contrast to the datasets analyzed in A21 (and references

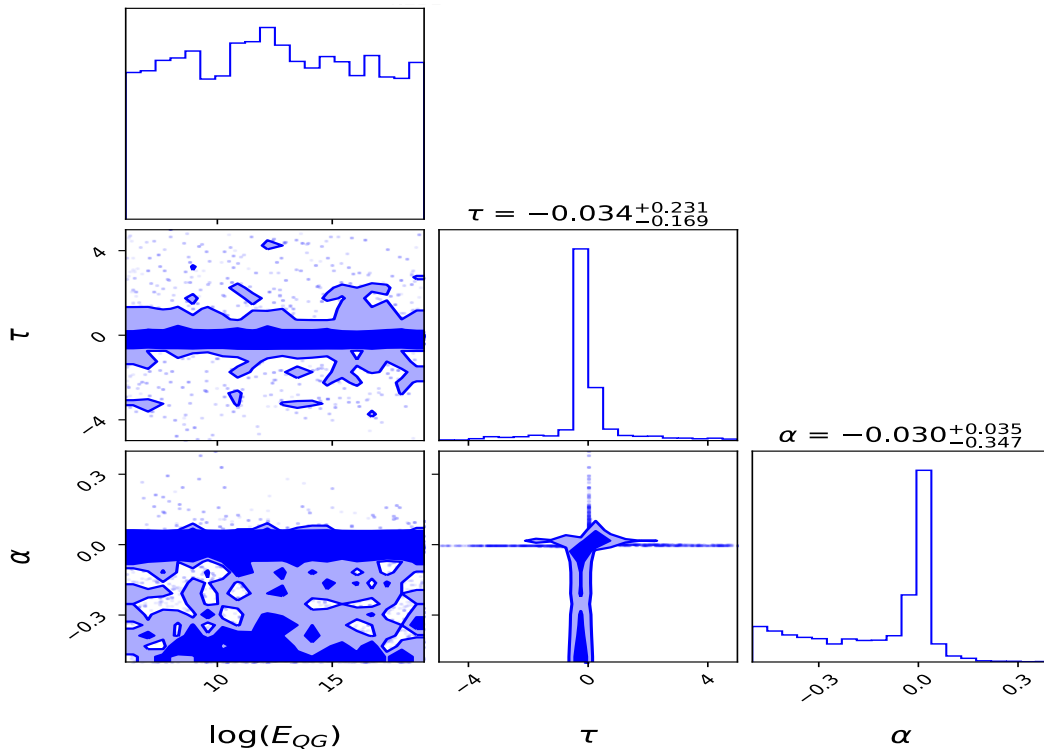


FIG. 3: The marginalized 68% and 90% credible regions for the quadratic LIV model, corresponding to $n = 2$ in Eq. 4. Since, no closed contour for E_{QG} is obtained (similar to Fig. 2), we only set lower limits on E_{QG} , given by $E_{QG} > 6.8 \times 10^9$ GeV at 95% c.l.

therein), which showed strong or decisive significance for LIV as compared to only intrinsic-induced lags.

-
- [1] S. Xiao, S. L. Xiong, S. N. Zhang, L. M. Song, F. J. Lu, Y. Huang, C. Cai, Q. B. Yi, X. Y. Song, W. Chen, et al., *Astrophys. J.* **920**, 43 (2021).
- [2] G. Amelino-Camelia, J. Ellis, N. E. Mavromatos, D. V. Nanopoulos, and S. Sarkar, *Nature (London)* **395**, 525 (1998).
- [3] Y. Pan, J. Qi, S. Cao, T. Liu, Y. Liu, S. Geng, Y. Lian, and Z.-H. Zhu, *Astrophys. J.* **890**, 169 (2020), 2001.08451.
- [4] G. Amelino-Camelia, J. Ellis, N. E. Mavromatos, D. V. Nanopoulos, and S. Sarkar, *Nature (London)* **393**, 763 (1998), astro-ph/9712103.
- [5] J. Ellis, N. E. Mavromatos, D. V. Nanopoulos, and A. S. Sakharov, *Astron. & Astrophys.* **402**, 409 (2003), astro-ph/0210124.
- [6] J. Ellis, N. E. Mavromatos, D. V. Nanopoulos, A. S. Sakharov, and E. K. G. Sarkisyan, *Astroparticle Physics* **25**, 402 (2006), astro-ph/0510172.
- [7] A. A. Abdo, M. Ackermann, M. Ajello, K. Asano, W. B. Atwood, M. Axelsson, L. Baldini, J. Ballet, G. Barbiellini, M. G. Baring, et al., *Nature (London)* **462**, 331 (2009), 0908.1832.

- [8] Z. Chang, X. Li, H.-N. Lin, Y. Sang, P. Wang, and S. Wang, *Chinese Physics C* **40**, 045102 (2016), 1506.08495.
- [9] V. Vasileiou, A. Jacholkowska, F. Piron, J. Bolmont, C. Couturier, J. Granot, F. W. Stecker, J. Cohen-Tanugi, and F. Longo, *Phys. Rev. D* **87**, 122001 (2013), 1305.3463.
- [10] V. Vasileiou, J. Granot, T. Piran, and G. Amelino-Camelia, *Nature Physics* **11**, 344 (2015).
- [11] S. Zhang and B.-Q. Ma, *Astroparticle Physics* **61**, 108 (2015), 1406.4568.
- [12] Y. Liu and B.-Q. Ma, *European Physical Journal C* **78**, 825 (2018), 1810.00636.
- [13] Y. Pan, Y. Gong, S. Cao, H. Gao, and Z.-H. Zhu, *Astrophys. J.* **808**, 78 (2015), 1505.06563.
- [14] H. Xu and B.-Q. Ma, *Physics Letters B* **760**, 602 (2016), 1607.08043.
- [15] H. Xu and B.-Q. Ma, *Astroparticle Physics* **82**, 72 (2016), 1607.03203.
- [16] J.-J. Wei and X.-F. Wu, *Astrophys. J.* **851**, 127 (2017), 1711.09185.
- [17] S. Ganguly and S. Desai, *Astroparticle Physics* **94**, 17 (2017), 1706.01202.
- [18] J. Ellis, R. Konoplich, N. E. Mavromatos, L. Nguyen, A. S. Sakharov, and E. K. Sarkisyan-Grinbaum, *Phys. Rev. D* **99**, 083009 (2019), 1807.00189.
- [19] J.-J. Wei, *Mon. Not. R. Astron. Soc.* **485**, 2401 (2019), 1905.03413.
- [20] S.-S. Du, L. Lan, J.-J. Wei, Z.-M. Zhou, H. Gao, L.-Y. Jiang, B.-B. Zhang, Z.-K. Liu, X.-F. Wu, E.-W. Liang, et al., *Astrophys. J.* **906**, 8 (2021), 2010.16029.
- [21] V. A. Acciari et al. (MAGIC, Armenian Consortium: ICRArNet-Armenia at NAS RA, A. Alikhanyan National Laboratory, Finnish MAGIC Consortium: Finnish Centre of Astronomy with ESO), *Phys. Rev. Lett.* **125**, 021301 (2020), 2001.09728.
- [22] X.-B. Zou, H.-K. Deng, Z.-Y. Yin, and H. Wei, *Physics Letters B* **776**, 284 (2018), 1707.06367.
- [23] R. Agrawal, H. Singirikonda, and S. Desai, *JCAP* **2021**, 029 (2021), 2102.11248.
- [24] D. J. Bartlett, H. Desmond, P. G. Ferreira, and J. Jasche, *Phys. Rev. D* **104**, 103516 (2021), 2109.07850.
- [25] J.-J. Wei and X.-F. Wu, *Frontiers of Physics* **16**, 44300 (2021), 2102.03724.
- [26] Z.-K. Liu, B.-B. Zhang, and Y.-Z. Meng, *arXiv e-prints arXiv:2202.09999* (2022), 2202.09999.
- [27] S. Xiao, S.-L. Xiong, Y. Wang, S.-N. Zhang, H. Gao, Z. Zhang, C. Cai, Q.-B. Yi, Y. Zhao, Y.-L. Tuo, et al., *Astrophys. J. Lett.* **924**, L29 (2022).
- [28] P. Kumar and B. Zhang, *Physics Reports* **561**, 1 (2015), 1410.0679.
- [29] A. Singh and S. Desai, *JCAP* **2022**, 010 (2022), 2108.00395.
- [30] C. Kouveliotou, C. A. Meegan, G. J. Fishman, N. P. Bhat, M. S. Briggs, T. M. Koshut, W. S. Paciesas, and G. N. Pendleton, *Astrophys. J. Lett.* **413**, L101 (1993).
- [31] S. E. Woosley and J. S. Bloom, *Ann. Rev. Astron. Astrophys.* **44**, 507 (2006), astro-ph/0609142.
- [32] E. Nakar, *Physics Reports* **442**, 166 (2007), astro-ph/0701748.
- [33] S. Kulkarni and S. Desai, *Astrophys. and Space Science* **362**, 70 (2017), 1612.08235.
- [34] A. Bhave, S. Kulkarni, S. Desai, and P. K. Srijith, *Astrophys. and Space Science* **367**, 39 (2022), 1708.05668.
- [35] T.-P. Li, J.-L. Qu, H. Feng, L.-M. Song, G.-Q. Ding, and L. Chen, *ChJAA* **4**, 583 (2004), astro-ph/0407458.
- [36] A. Krishak and S. Desai, *JCAP* **2020**, 006 (2020), 2003.10127.
- [37] J.-J. Wei and X.-F. Wu, *Frontiers of Physics* **16**, 44300 (2021), 2102.03724.
- [38] S. Sharma, *Ann. Rev. Astron. Astrophys.* **55**, 213 (2017), 1706.01629.
- [39] M. Kerscher and J. Weller, *SciPost Physics Lecture Notes* **9** (2019), 1901.07726.
- [40] J.-J. Wei, B.-B. Zhang, L. Shao, X.-F. Wu, and P. Mészáros, *Astrophys. J. Lett.* **834**, L13 (2017), 1612.09425.
- [41] L. Shao, B.-B. Zhang, F.-R. Wang, X.-F. Wu, Y.-H. Cheng, X. Zhang, B.-Y. Yu, B.-J. Xi, X. Wang, H.-X. Feng, et al., *Astrophys. J.* **844**, 126 (2017), 1610.07191.
- [42] U. Jacob and T. Piran, *JCAP* **1**, 031 (2008), 0712.2170.
- [43] N. Aghanim et al. (Planck), *Astron. Astrophys.* **641**, A6 (2020), 1807.06209.
- [44] M. Seikel, C. Clarkson, and M. Smith, *JCAP* **1206**, 036 (2012), 1204.2832.
- [45] R. Jimenez and A. Loeb, *Astrophys. J.* **573**, 37 (2002), astro-ph/0106145.
- [46] H. Singirikonda and S. Desai, *European Physical Journal C* **80**, 694 (2020), 2003.00494.
- [47] K. Bora and S. Desai, *JCAP* **2021**, 052 (2021), 2104.00974.
- [48] R. Trotta, *ArXiv e-prints* (2017), 1701.01467.
- [49] A. Krishak, A. Dantuluri, and S. Desai, *JCAP* **2020**, 007 (2020), 1906.05726.
- [50] S. Bhagvati and S. Desai, *JCAP* **2021**, 022 (2021), 2106.06724.
- [51] J. S. Speagle, *Mon. Not. R. Astron. Soc.* (2020), 1904.02180.